The effects of meltwater percolation on the seasonal isotopic signals in an Arctic snowpack

Tara MORAN, Shawn MARSHALL

Department of Geography, University of Calgary, 2500 University Drive NW, Calgary, Alberta T2N 1N4, Canada
E-mail: tamoran@ucalgary.ca

ABSTRACT. We investigate the evolution of snow temperature, water content, density and stable water isotopes of $\delta^{18}O$ at four Arctic snow-pit sites during early-season melt, in order to understand the effects of melt on snowpack stratigraphies and seasonal isotopic signals. We relate isotopic changes observed at these sites to temperature reconstructions derived from a 33 year firn-core record drilled on the same icefield. Decreases in seasonal isotopic amplitudes observed at all but one snow-pit site coincide with the percolation of more enriched meltwater into the snowpack, suggesting that meltwater percolation is the dominant process causing isotopic redistribution in Arctic snowpacks during the melt season. The decrease in isotopic range was accompanied by increases in mean $\delta^{18}O$ values at all snow-pit sites. Positive degree-day (PDD) calculations are used to relate the amount of melt observed at the low-elevation snow-pit sites to the firn-core site. Results based on PDD values suggest an average overestimation of 1.1°C in average annual temperature reconstructions from the firn-core site from 1967 to 2006, with the possibility of errors in excess of 3°C during high-melt years.

INTRODUCTION

Stable water isotope ratios ($\delta^{18}O$, $\delta^{2}H$) in ice-core records from both the Greenland and Antarctic ice sheets have demonstrated the ability to elicit high-resolution proxy records for air temperature (Dansgaard and others, 1993; Petit and others, 1999). However, isotopic information stored in individual precipitation events could be modified by various processes, including wind scour (Fisher and Koerner, 1994), meltwater percolation (Taylor and others, 2001; Unnikrishna and others, 2002), erosive and depositional sublimation (Friedman and others, 1991; Stichler and others, 2001), meltwater refreezing (Zhou and others, 2008) and vapour diffusion (Johnsen and others, 2000).

Many ice-core studies acknowledge the potential of meltwater percolation to affect the accuracy of palaeoclimatic reconstructions (Jouzel and others, 1997; Koerner, 1997; Schotterer and others, 2004). Meltwater percolation can cause the reduction of seasonal isotopic signals (Pohjola and others, 2002), isotopic enrichment, the introduction of time gaps (Koerner, 1997) and the elution of chemical species (Moore and others, 2005). As a result, care should be taken when deriving climatic information from ice cores drilled in areas that experience high amounts of summertime melt. Studies focusing on the effects of chemical species in ice-core records with melt indices as high as 80% have found that chemical signals within the core are preserved at annual to biannual resolution (Grumet and others, 2001; Moore and others, 2005).

Pohjola and others (2002) and Goto-Azuma and others (2002) investigated the effects of meltwater percolation on stable water isotopes from Arctic ice cores. Both studies acknowledge the reduction of seasonal isotopic values accompanying meltwater percolation; however, the similarity between annual $\delta^{18}O$ values from an ice-core site and adjusted coastal values led Pohjola and others (2002) to conclude that there are no significant changes to mean annual isotopic values resulting from average melt values of 55%. These results contrast with those of Goto-Azuma and others (2002), who found significant evidence of post-depositional modification of $\delta^{18}O$ signals resulting from melt. As a result of these findings, Goto-Azuma and others (2002) limit the use of $\delta^{18}O$ signals to a combined $\delta^{18}O$–melt record temperature proxy.

The potential for isotopic fractionation resulting from refreezing of meltwater within the snowpack (Zhou and others, 2008) and the enrichment of isotopic species from increased evaporation and sublimation during periods of melt (Stichler and others, 2001) could impact the ability of isotopic values to serve as accurate proxies of environmental change. This study seeks to quantify the effects of meltwater percolation on isotopic species in low-elevation snow pits sampled prior to melt and during the early melt season, with the goal of estimating the effects of meltwater percolation on annual temperature reconstructions at a high-elevation firn-core site located on the same icefield.

The Prince of Wales (POW) Icefield, located at 78.48° N, 79.43° W, Ellesmere Island, Nunavut, Canada, has an area of 19 325 km², with a broad, gently sloping central plateau ranging in altitude from 1400 to 1730 m (Fig. 1). In spring 2001, a 20 m firn core was collected from the interior plateau of the icefield (1727 m) (Fig. 1b). Annual-layer counting of $\delta^{18}O$ and sulphate peaks was used to develop a firn-core chronology, which spans 33 complete years, 1967–99. This record is relatively short, but increases in frequency and per cent of annual ice content indicate that melt on the plateau has increased since the mid-1970s. At present we do not understand the impact of these intermittent melt events on the isotopic record preserved in the POW firn-core record, and are unable to assess the viability of this site as a long-core drill site. Quantification of meltwater-induced isotope modification is therefore needed to ensure the validity of palaeoclimatic reconstructions from this and other ice-core sites subject to summertime melt. This research is expected to become increasingly relevant as high northern latitudes experience dramatic warming (Solomon and others, 2007).

We returned to the POW Icefield in spring 2007 to examine the impact of meltwater on the isotopic composition of $\delta^{18}O$ at snow-pit sites on Leffert Glacier, a large outflow
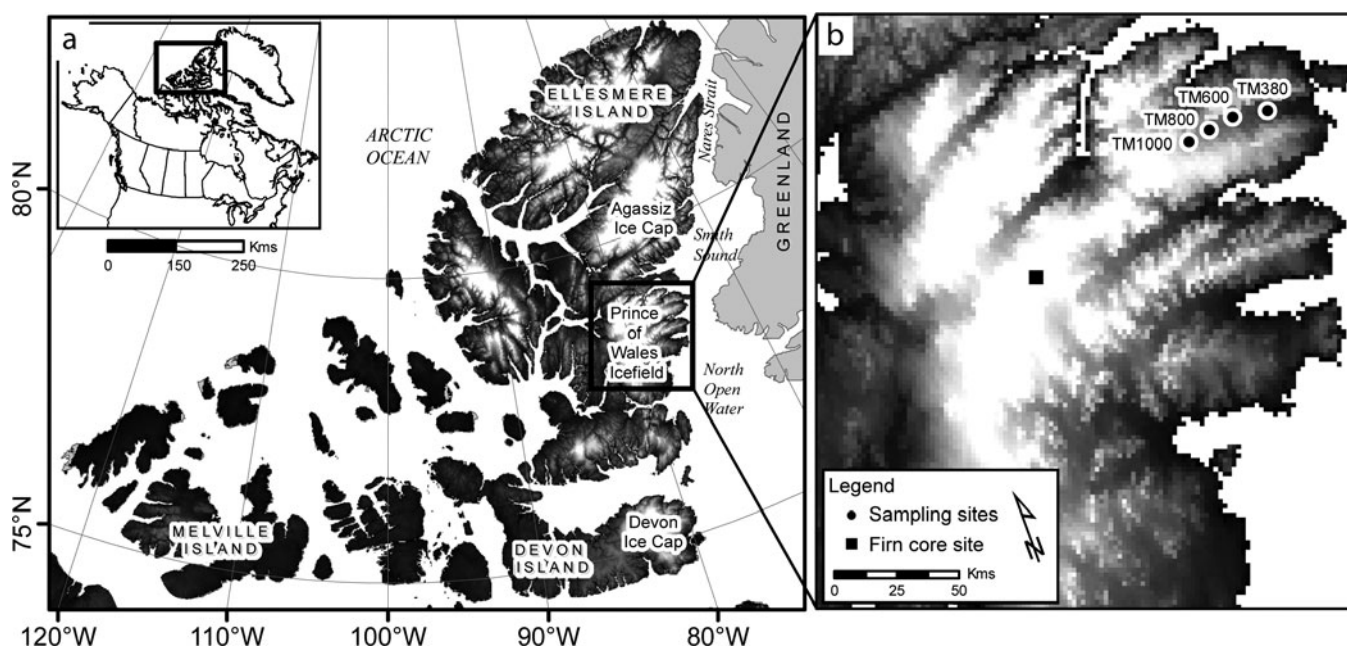
Fig. 1. (a) Location of the POW Icefield, Nunavut, Canada. (b) Snow-pit sampling sites at 380, 600, 800 and 1000 m a.s.l. (labelled TM380, TM600, TM800 and TM1000, respectively) on Leffert Glacier, POW Icefield. The firn-core site is also shown.

glacier of the POW Icefield. Because melt is not guaranteed at the firn-core drill site in a given summer, four snow-pit sites were established at elevation intervals of ∼200 m, along a low-elevation transect from 380 to 1000 m (Fig. 1b). Sampling sites are referred to as TM380, TM600, TM800 and TM1000, indicating their elevation. Each site was sampled a minimum of six times over the course of the study; as a result, individual snow pits at a specific location are referred to by both the site name and pit number (e.g. TM380 pit 1). Having sites along an altitudinal gradient ensured that melt conditions were observed during our study and allowed comparison of sites experiencing varying degrees of melt. Fieldwork for this study was conducted early in the melt season to ensure that snow-pit sites were first sampled prior to the onset of melt, and to ensure safe snowmobile travel along the sampling transect.

EXPERIMENTAL SET-UP

All snow-pit sites were located in the ablation zone of the glacier and were dug to glacial ice. Snow begins to accumulate at lower-elevation sites on the POW Icefield in late August/early September and continues until late May/early June, when the melt season begins (Marshall and others, 2007). Snow-pit stratigraphies from the four sampling sites had an average depth of 43.7 cm, which represents the autumn through spring accumulation season (i.e. September until the time of sampling; Table 1). For the duration of the study, each snow-pit site was equipped with a temperature/relative-humidity sensor, recording data at 4 min intervals. Sensors were encased in a Stephenson screen ∼1.5 m off the snow surface.

To establish baseline conditions for each site, all snow-pit sites were sampled before daily maximum temperatures reached 0°C. These pits are referred to as pre-melt snow pits. After the onset of melt, snow pits were sampled every 2 days for snow water content, temperature, density and stable water isotopes ($\delta^{18}O$). Dye pits and detailed snow-pit

stratigraphies looking at snow type, grain size, hardness and ice-lens location and thickness were also performed at each visit.

At TM800 and TM1000, after the pre-melt snow pit was sampled, all subsequent snow pits were cut back ∼20 cm from the previous pit's rear wall to minimize variations in snow-pit depths, while ensuring undisturbed snow-surface conditions. Pits were not back-filled between sampling visits, but filling of the pits through wind deposition between sampling visits is thought to have minimized temperature perturbations on the snow-pit wall. The procedure of cutting snow pits back from the previous pit's rear wall was not initiated until the third visit to sites TM380 and TM600, which were equipped with time-domain reflectometer (TDR) probes on the first visit and both TDR probes and thermistors on the second visit. The first and second snow pits were therefore dug and sampled at the same location, but subsequent snow pits at these sites were dug ∼1.5 m away from the original snow-pit site, in order to ensure probes were not disturbed. We acknowledge that sampling in a sightly different location may result in the measurement of different snow profiles. We address this potential for error below. Snow samples were collected every 5 cm vertically in the snowpack with a $5 \times 5 \times 4$ cm (100 cm^3) stainless-steel snow sampler, making for near-continuous sampling. Samples were taken from shaded snow-pit walls in order to minimize the influence of solar radiation.

Variations in snowpack depth were observed at all sites over the course of the study and are presumed to be the result of differences in settling rate during the densification process, local-scale differences in accumulation rate, wind deposition and erosion, and variations in the underlying glacial topography at individual sampling sites. Plots of snow-pit stratigraphic profiles at individual sampling sites indicate that stratigraphic layers maintain the same structure regardless of depth. snow-pit depths are converted to snow water equivalent (SWE) to minimize the effects of densification and are normalized to adjust for spatial variability in depth. All

Table 1. Sample dates; mean density-weighted $\delta^{18}O$ values; mean, maximum and minimum $\delta^{18}O$ ranges (defined as the difference between the minimum and maximum $\delta^{18}O$ values within each snow pit); per mil changes in $\delta^{18}O$ and $\delta^{18}O$ ranges ($\Delta\delta^{18}O$ and Δrange); and positive degree-day (PDD) values for all snow-pit sites. PDD values were calculated using 4 min sampled temperature data from each snow-pit site. Bold and italicized values are significant at the 95% and 90% confidence levels, respectively

Site	Sample dates	$\delta^{18}O$	$\delta^{18}O$ range			$\Delta\delta^{18}O$	Δrange	PDD
			Mean	Max	Min			
		‰	‰	‰	‰	‰	‰	°C d
TM380	29 May to 14 June	−26.7	13.7	15.0	11.6	0.4	**−3.0**	7.5
TM600*	8 June to 16 June	−25.7	9.2	9.8	8.3	*2.6*	*−1.4*	5.5
TM800	30 May to 16 June	−28.8	12.3	15.0	11.0	0.1	−2.2	3.7
TM1000†	7 June to 16 June	−29.2	13.9	15.3	9.6	*2.5*	0.4	1.6

*Excludes dates and values from pits 1 and 2 (see notes in text).
†Excludes dates and values from pit 1 (see notes in text).

snow-pit-averaged isotopic values presented in the analysis have been density-weighted.

Instrumentation

Snow temperature was measured with a digital thermometer ($\pm 0.2°C$) for each 5 cm sampling layer. Water volume content was derived from dielectric permittivity measurements using a flat capacitance sensor (20 MHz, $\pm 3\%$ volumetric water content (Denoth, 1994; Eller and Denoth, 1996). Samples were weighed to the nearest 0.1 g using a digital scale and subsequently converted to snow densities (kg m^{-3}). The average analytical error resulting from uncertainty in sample volumes and weighing is estimated to be ± 30 kg m^{-3}.

Samples were thawed and bottled, without headspace, in 25 mL double-lidded HDPE sample bottles. Samples were stored in a refrigerator prior to laboratory analysis to minimize evaporation. All samples were analysed for isotopic ratios using a Thermo Finnigan mass spectrometer with a glassy carbon reactor optimized for simultaneous analysis of both $\delta^{18}O$ and δ^2H by the conversion of H_2O to H_2 and CO, with sampling errors of ± 0.2 and ± 1.0‰, respectively.

Total sampling error for density and isotope samples is the sum of both analytical error and sampling error. Analytical error is defined as error resulting from instrumental uncertainty, as outlined by instrument manufacturers and laboratory protocol (reported above). Sampling error refers to the repeatability of field measurements and is dominated by spatial variability in the snowpack stratigraphy. Sampling across horizontal strata in a snow pit should only introduce minor variations in density and isotopic ratios, resulting from local variations in wind redistribution, differences in glacier and snow-surface topography, dipping strata and local-scale variations in snow accumulation. In order to quantify sampling variations in density and isotopic ratios, three replicate samples were taken along horizontal strata during the sampling of each snow pit.

The sampling errors for both density and isotope ratios are averaged across all error samples from all snow pits, with the assumption that these errors are representative of local-scale processes at all sites across time. Average sampling error is estimated to be ± 0.5 and ± 3.8‰ for $\delta^{18}O$ and δ^2H, and ± 17 kg m^{-3} for snow density; giving *total* error estimates of ± 0.7, ± 4.8‰ and ± 47 kg m^{-3}, respectively. Error bars displayed in snow-pit profiles of snow density and

isotopic values are total error estimates. Note that these error estimates refer to point samples within the stratigraphy; the error is greatly reduced for depth-averaged isotopic values in the snowpack (scaled by $1/\sqrt{N}$, where N is the number of samples).

At TM380 and TM600, averaged in situ snow temperatures were recorded every 30 min from samples measured every 10 s, using 44002A thermistors from Yellow Springs Instruments. Thermistors were located every 5 cm vertically in the snowpack, beginning 3 cm below the snow surface. All thermistors were calibrated in an ice bath. Two sensors were found to have biases of $+0.3°C$. All data presented here have been corrected to account for this bias. Manufacturer instrument accuracy is reported to be $\pm 0.2°C$ for temperatures from 0 to 70°C. While the manufacturer states that these thermistors are stable for temperatures from –80 to 50°C, their accuracy below 0°C is not given.

Sites TM380 and TM600 were equipped with TDR probes taking hourly water-content measurements. While traditionally developed to measure water content in soil and rock, these probes have been used in more recent years to measure water content and density in snowpacks (Schneebeli and others, 1998; Waldner and others, 2004). The data derived from these probes are not presented here because the pre-melt water-content measurements had a large degree of sampling variation. These variations are probably due to the low density values of the thin Arctic snowpack and formation of air pockets around the probes. However, after melt onset, and the subsequent densification of the snowpack, the sensors in the upper portion of the snowpack showed strong diurnal variation in meltwater content, consistent with water-content values derived from the capacitance sensor. These sensors may be of great value to meltwater studies extending beyond the beginning of the melt season, and we recommend further exploration of TDR probes for studies of meltwater percolation in low-density snowpacks.

RESULTS

The results presented here focus on our lowest-elevation sampling site, TM380, which experienced the most melt during the study. TM380 was sampled a total of six times during the 16 day study period (Fig. 2). The pre-melt snow pit was sampled prior to the onset of melt, as indicated by the snow temperatures measured in pit 1, which had a maximum temperature of –5.7°C (Fig. 3a). Over the 16 day
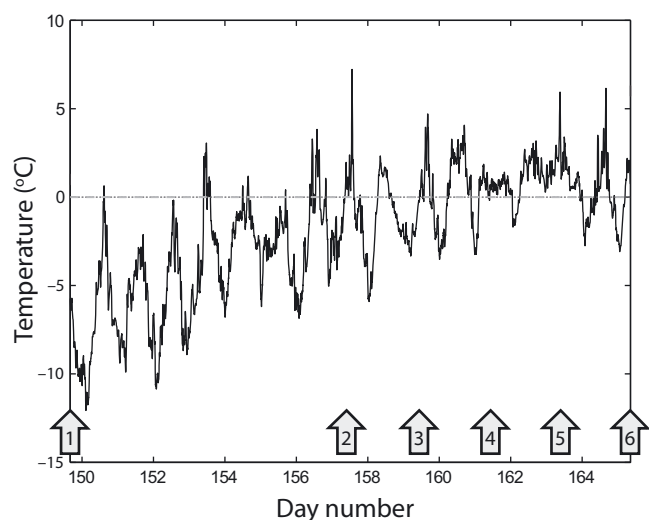
Fig. 2. Air temperature at the TM380 snow-pit sampling site from 29 May to 14 June 2007. The numbered arrows indicate the date each snow pit was sampled.

study period the air temperature at TM380 increased from a mean daily temperature of –6.6°C to 0.0°C. A maximum air temperature of 7.6°C was recorded on 6 June (day 157). In addition to the warming trend observed at TM380 over the course of the study, there is a strong diurnal temperature signal, with nighttime temperatures dropping below freezing throughout the study period (Fig. 2). These conditions are typical of high-summer conditions at the firn-core site on the icefield plateau.

Snow temperature, water content and density

Figure 3 plots the progression of snow temperature, water content and density values at TM380 over the course of the study. Average snow temperatures increase from –9.1°C in pit 1 to –1.5°C in pit 6 (Fig. 3a). From pit 1 to pit 3 there is an increase in snow temperature observed throughout the entire snow-pit profile, with surface snow temperatures in pit 3 reaching 0°C. Subsequent snow pits show a downward propagation of the 0°C isotherm, corresponding with increases in the water content (Fig. 3b). These results are similar to previous studies by Conway and Benedict (1994) and Pfeffer and Humphrey (1996), who used the position of the 0°C isotherm to track the movement of meltwater through a melting snowpack.

Water content and snow density at TM380 do not change notably until pit 5. Consequently, plots of these parameters are simplified to show results only from pits 1, 4, 5 and 6. Water content increased from a mean value of 0.1% in the pre-melt snow pit to a mean value of 1.7% in pit 6. A maximum water content of 5.0% is observed in the surface layers of pit 5 (Fig. 3b), with a visibly moist snow layer occurring immediately above an ice layer (Fig. 4, pit 5).

Mean snow-pit densities at TM380 increase from 256 kg m^{-3} in pit 1 to 277 kg m^{-3} in pit 6 (Fig. 3c). Corresponding to observed changes in water content, there is a sharp increase in snow densities in the upper layers of the snowpack from pit 4 to pit 5. The average density in the upper third of the snow pits increases 27% from 311 kg m^{-3} in pit 1 to 394 kg m^{-3} in pit 6.
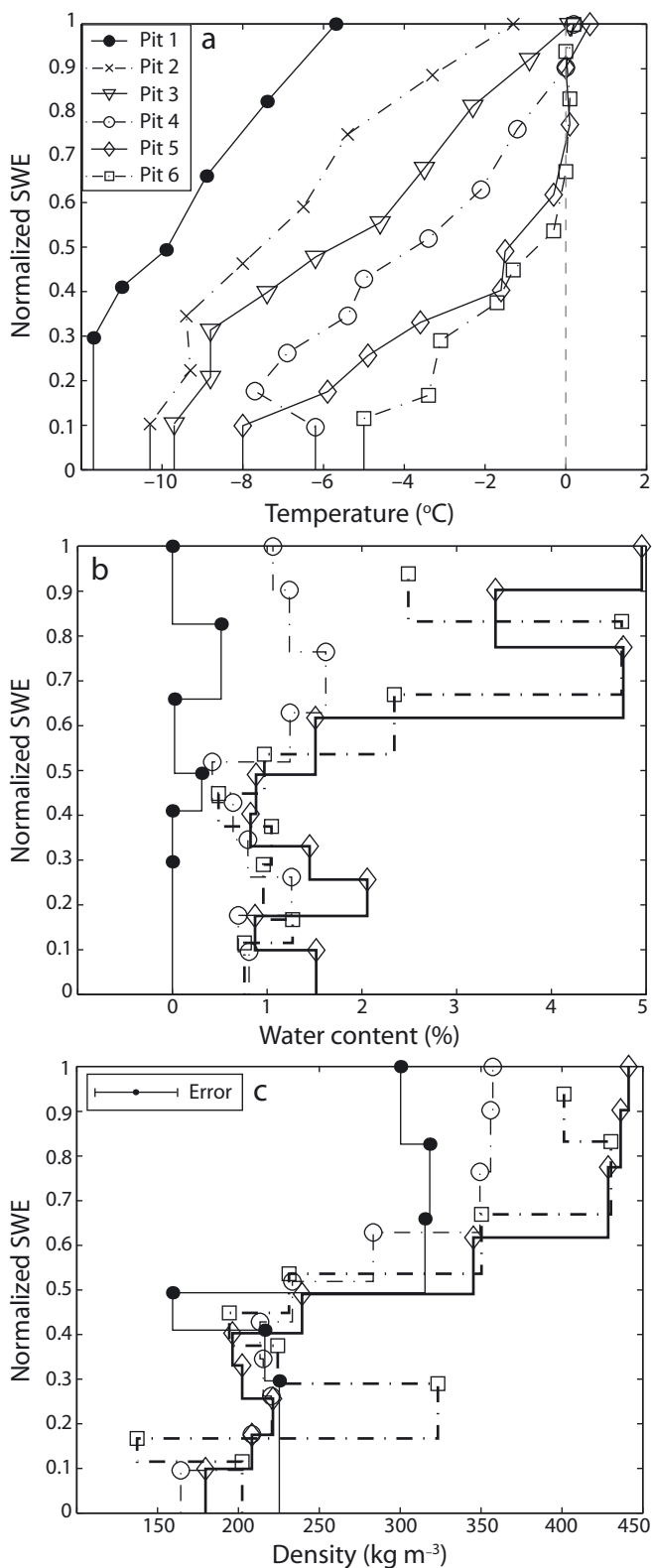
Fig. 3. (a) Snow-pit temperatures for all TM380 snow pits, (b) per cent water content and (c) density, for TM380 pits 1, 4, 5 and 6. The legend in (a) also applies to (b) and (c). Error bars are not shown for snow temperature and water content, which have estimated errors of 0.2°C and 3%. A normalized SWE value of 1 represents the snow surface; glacial ice is 0.

Snow-pit stratigraphies

Snow-pit stratigraphies for all TM380 snow pits are shown in Figure 4. Snow types from these and stratigraphies performed at other sampling sites over the course of the study,
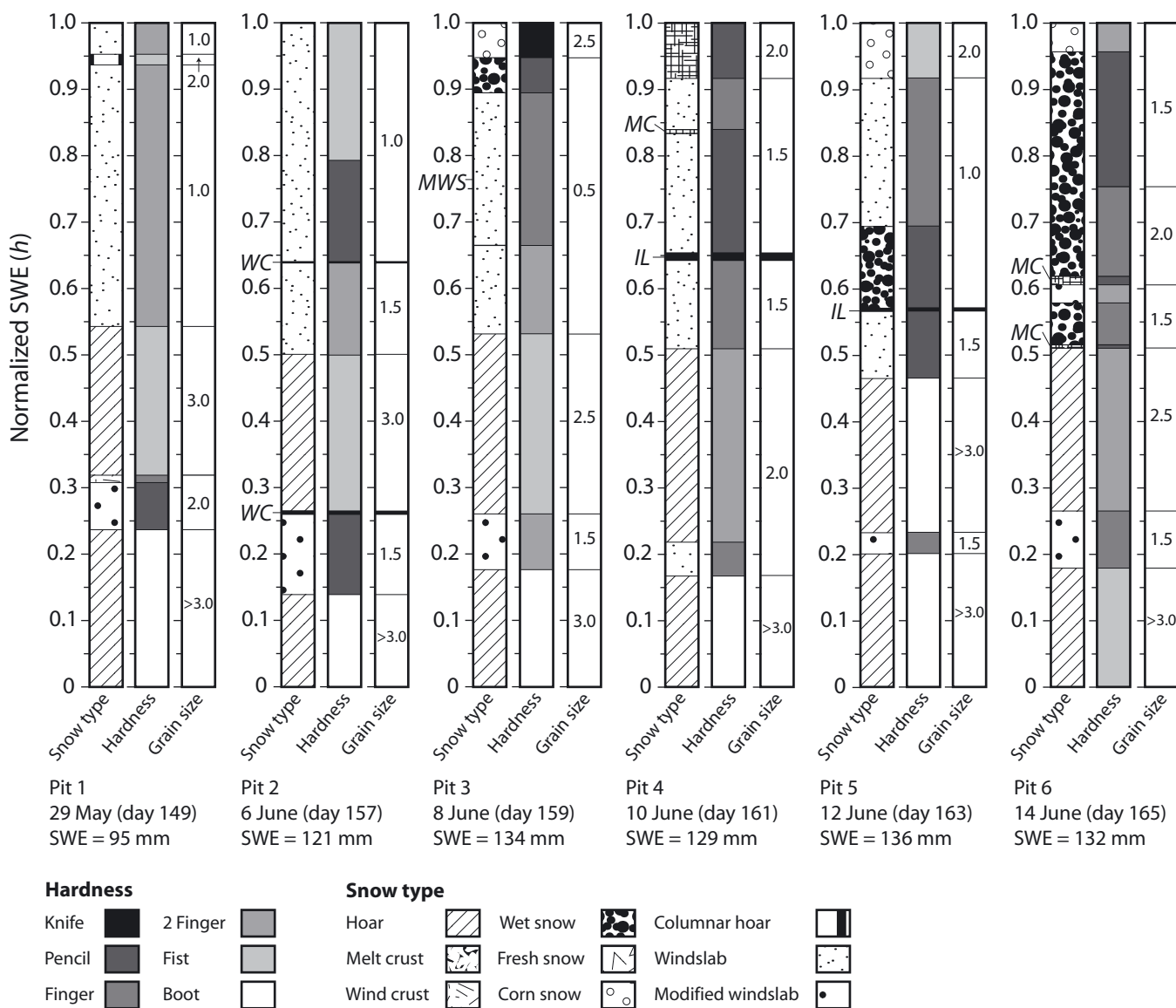
Fig. 4. Snow-pit stratigraphies including snow type, hardness and grain size (mm) for all snow pits sampled at TM380. IL is ice layer, MWS is moist windslab, WC is wind crust and MC is melt crust. A normalized SWE value of 1 represents the snow surface; glacial ice is 0.

can be divided into three broad categories: (1) hoar-frost, accumulating in autumn and early winter, (2) wintertime windslab, punctuated with thin wind crusts, and (3) fresh springtime snow. All snow-pit sites show a strong seasonal isotopic signal, with minimum $\delta^{18}O$ values occurring within the fine-grained (~1.0 mm) winter layers.

At TM380, snow grain size increased over the 16 day study from an initial average of 1.0 mm to a grain size of 1.5–2.0 mm. Qualitative measures of snow hardness show increases throughout the entire snow-pit profile. The largest changes were observed in the top half of the snow pit, where hardness increased from 2 finger/finger to finger/pencil. These results are consistent with the increases observed in snow-pit densities.

Two types of ice layers formed during this study: (1) continuous layers of solid ice without visible crystal structure and (2) more permeable ice layers, with discernible crystal structure. We refer to these as 'ice layers' and 'melt crusts', respectively. A total of four ice layers and nine melt crusts were identified at all snow-pit sites over the course of the study. All but one formed at previously identified

transitions in snow type, hardness or grain size. Three of the melt crusts formed from previously identified ice layers as melt progressed.

By the end of the study the upper 75% of the snowpack had reached temperatures of 0°C, but overnight refreezing and cooling were measured to 13 cm depth, or a normalized SWE (h) value of 0.65 (T3). Similar results were found in the snow-pit stratigraphies at TM600 (not shown). The diurnal variations in air temperature play an important role in nighttime refreezing and the formation of ice layers in the upper layers of the snowpack. Nightly refreezing of meltwater in the snowpack slows progression of melt at these sites, as a large amount of heat energy at the onset of melt must be devoted to warming the snowpack and re-thawing these ice layers before 'new' melt can proceed.

In the case of TM380, the wind crust at a normalized SWE (h) value of 0.64 in pit 2 (Fig. 4) influences both the percolation of meltwater and the location of ice layers within the snow-pit stratigraphy. These effects can be tracked through the visual snow-pit stratigraphies (Fig. 4) and in the thermistor data (Fig. 5b).
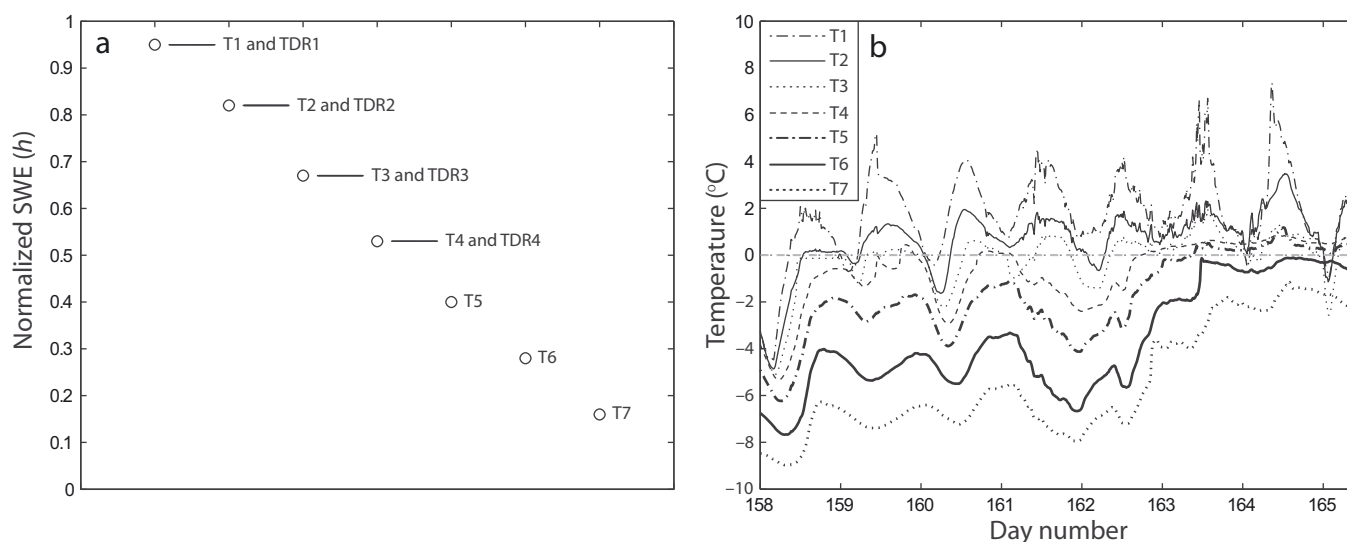
Fig. 5. (a) Initial location of thermistors and TDR probes in the TM380 snow-pit profile. (b) snow-pit temperatures from thermistors at the TM380 snow-pit sampling site from 7 to 14 June 2008. A normalized SWE value of 1 represents the snow surface; glacial ice is 0.

The ice layer observed in pits 4 and 5 ($h = 0.65$ and 0.57, respectively) is thought to be the same ice layer, as it falls within the degree of variability associated with snow-pit SWE at this site (average cumulative SWE for this site is 124.6 ± 15.4 mm, giving a normalized SWE of 1.0 ± 0.1). This ice layer was ~4 mm thick at the time of formation and occurred at the location of the wind crust identified in pit 2. The ice layer identified in pits 4 and 5 persists in pit 6 as a more breakable melt crust ($h = 0.62$). A second melt crust is observed to form in pit 6 ($h = 0.51$), at a previously identified transition between windslab and hoar layers. The highest water contents observed in TM380 stratigraphies occur immediately above ice and melt crust layers (Fig. 4, pits 5 and 6).

Figure 5a shows the location of the seven thermistors (T1–T7) and four TDR probes (TDR1–TDR4) within the snowpack profile at TM380, with the temperature data from each thermistor probe plotted in Figure 5b. It is commonly acknowledged that temperature sensors as deep as 20 cm below the snow surface can be affected by the penetration of radiation through the snowpack (Pfeffer and Humphrey,

1996). While thermistors were covered in white shrink wrap to limit the amount of direct heating resulting from radiative penetration, the >0°C temperatures observed by T1–T3 indicate that it remained a factor. These sensors were not removed from the analysis however, because their records still provide insight into the large diurnal variations observed in snow-pit temperatures at TM380 over the course of the study (Fig. 5b).

The progression of meltwater percolation can be tracked through the snow-pit profile using the location of the 0°C isotherm. In situ temperatures for T2 and T3 ($h = 0.82$ and 0.67) are observed to stay at a temperature of ~0°C on the evening of 7/8 June (day 158/159; Fig. 5b), while surrounding thermistors show a more classic diurnal temperature trend. This observation corresponds with the percolation of meltwater to $h = 0.67$ in the snow-pit stratigraphy (Fig. 4, pit 3).

On 9/10 June (day 160/161) at TM380, T4 maintains a temperature of 0°C throughout the night, while decreasing temperatures are observed at T3. The timing of this observation corresponds with the formation of the 4 mm thick ice layer identified in pits 4 and 5. We believe this observation is related to the release of latent heat to the snowpack during ice-layer formation.
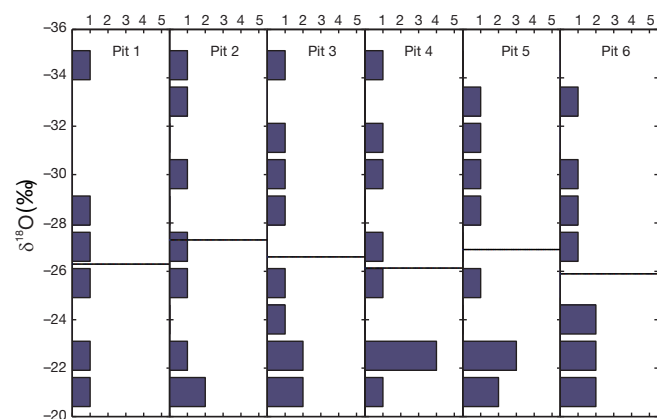
Isotopic values

The isotopic profiles from the TM380 snow pits become less variable as melt progresses (Fig. 6). The $\delta^{18}O$ values for the pre-melt snow-pit range from –20.3 to –35.3‰, with a density-weighted average of –26.3‰. (Fig. 6, pit 1). The final snow pit, pit 6, has $\delta^{18}O$ values ranging from –20.7 to –33.3‰, with a density-weighted average of –25.9‰ (Fig. 6, pit 6).

Mean density-weighted $\delta^{18}O$ values show an altitudinal gradient of $-0.4‰ (100 \, \mathrm{m})^{-1}$, with an average density-weighted $\delta^{18}O$ value (across all snow pits) of –26.7‰ at TM380 decreasing to –29.2‰ at TM1000 (Table 1). In addition to the altitudinal gradient, seasonal signals in $\delta^{18}O$ values are discernible at all four snow-pit sites (Fig. 7), with an average $\delta^{18}O$ range, defined as the difference between the minimum and maximum $\delta^{18}O$ value within each snow

Fig. 6. Histograms showing the frequency distribution of $\delta^{18}O$ values for the TM380 snow pits. The line in each plot indicates the density-weighted average $\delta^{18}O$ value for each snow pit.
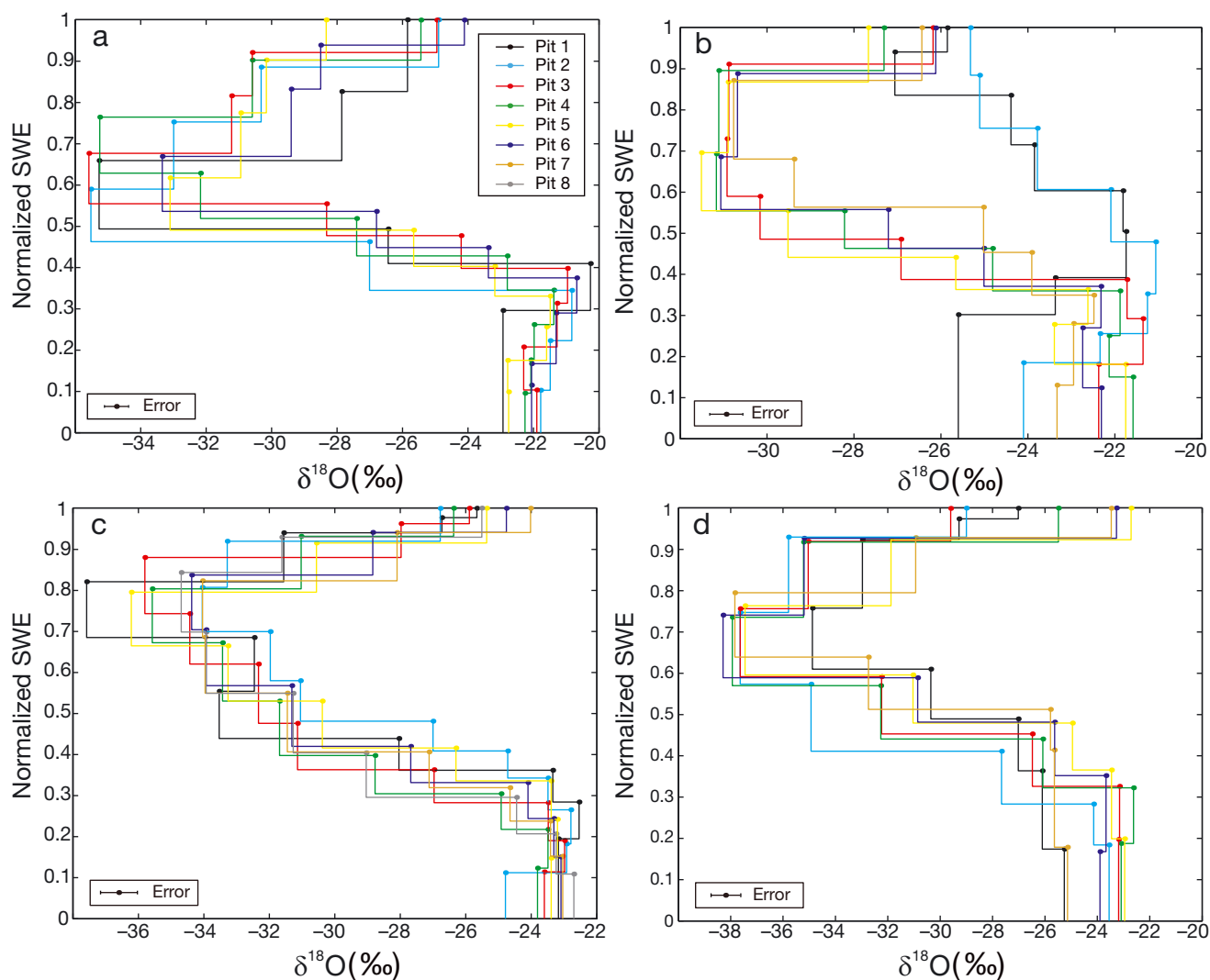
Fig. 7. $\delta^{18}O$ values for all snow-pit sites. (a) TM380; (b) TM600; (c) TM800; (d) TM1000. The legend in (a) applies to all of the snow-pit sites (except the error estimate, 0.7‰, which is the same for all sites, but is shown individually because of the differences in scale between the parts of the figure). A normalized SWE value of 1 represents the snow surface; glacial ice is 0.

pit, of 12.4‰. A maximum $\delta^{18}O$ range of 15.3‰ is observed in pit 4 of the TM1000 snow-pit site, and a minimum $\delta^{18}O$ range of 8.3‰ is seen in the final pit, pit 7, at TM600.

All snow-pit sites show an increase in average density-weighted $\delta^{18}O$ values over the course of the study (reported as positive $\Delta\delta^{18}O$ values in Table 1). Significant increases in $\delta^{18}O$ values are observed at the TM600 and TM1000 snow-pit sites; however, these sites are thought to have been influenced by fresh snowfall inputs (see below). Increases in mean $\delta^{18}O$ values at TM380 and TM800 are not statistically significant, but because fresh snowfall amounts at these sites were observed to be lower than at TM600 and TM1000 they are thought to be indicative of isotopic changes occurring as a result of melt processes. Even with a positive degree-day (PDD) value of $\leq7.5°C\,d$ (Table 1), increases in isotopic values are observed at all snow-pit sites, suggesting that isotopic enrichment has the potential to be significant under higher-melt scenarios.

Complications were observed in the TM1000 stratigraphies, as the minimum isotopic values observed in pits 2–7 were not captured in the pre-melt snow pit at this site (Fig. 7d). This discrepancy is probably the result of differences in snow-pit sampling location that occurred between pit 1 and subsequent sampling sites at this location.

Similar inconsistencies can be observed between the isotopic stratigraphies of pits 1 and 2 of TM600 and subsequent snow pits at this site. As described above, the first two snow pits sampled at TM600 were located ~1.5 m away from the sampling site established for pits 3–7, and are thought to have been sampled in an area where the winter snow was subject to wind redistribution. They show very similar isotopic profiles to one another, but not to subsequent sampling stratigraphies. Because of the complications observed in snow-pit stratigraphies, pits 2 and 3 were used as pre-melt (reference) snow pits for TM1000 and TM600, respectively.

Removal of pit 1 from the analysis increases the average isotopic range observed at TM1000 from 14.0‰ to 14.7‰, indicating that pit 1 did not capture the same seasonal isotopic range as other pits from the site. While similar improvements are observed at TM600, where average isotopic range increases from 7.9‰ to 9.2‰ with the removal of pits 1 and 2 from the analysis, the $\delta^{18}O$ ranges observed at the site (mean = 9.2‰) are consistently lower than at other snow-pit sites, which had an average $\delta^{18}O$ range of 13.5‰. Additional complications arise in the analysis as the reference snow pits from the TM600 and TM1000 sites may have experienced a small degree of melt. TM600 and TM1000 experienced 0.7 and 1.2 PDD by pit 3 and pit 2, respectively.

DATA ANALYSIS

Snow pits as an analogue for ice-core sites

PPD values are used to link isotopic modification observed at the low-elevation snow-pit sites with the amount of isotopic modification experienced at the firn-core site. The firn-core site has an average accumulation rate of 295 mm w.e. a^{-1}. Detailed snow-pit stratigraphies from the site performed during the 2007 field season indicate that surface melt produces intermittent but localized ice layers up to 1 cm thick. There is no indication that meltwater percolation at this site penetrates into the previous year's accumulation, although we cannot rule this out for exceptionally warm summers.

Historical PDD values

The firn-core site was equipped with an automated weather station (AWS) from 1 June 2001 to 23 September 2002, recording hourly temperature data. PDD values of 25.0 and 1.0°C d were derived for summers 2001 and 2002, respectively. Data in Table 1 indicate that snow-pit sampling sites in our study did not experience PDD values as high as those experienced at the firn-core site in 2001. The summers of 2001 and 2002 are thought to represent two extremes in melt conditions occurring at the firn-core site, with substantial melt observed in the summer of 2001 and no melt observed in the summer of 2002 (Marshall and others, 2007). The amount of melt observed at the snow-pit sites is therefore likely to represent more typical melt seasons experienced at the firn-core site.

To test this assumption, we estimate historical PDD values for the firn-core site as a means of assessing the average amount of melt and to compare these values with the amount of melt experienced at the snow-pit sites. Using the 2001 and 2002 AWS data, we evaluate PDD values derived for the same years using (1) eight-times-daily 2 m surface temperature data from the North American Regional Reanalysis (NARR) dataset, available on a ∼32 km resolution gridcell with data from 1979 to the present, and (2) four-times-daily surface and pressure level temperature data from the US National Centers for Environmental Prediction (NCEP), available on a 2.5° latitude–longitude grid from 1948 to the present. Data for both reanalysis datasets are available through the US National Oceanic and Atmospheric Administration's National Climatic Data Center at http://www.cdc.noaa.gov. The results from this comparison will provide the dataset most appropriate for calculating historical PDD values at the firn-core site.

Table 2 reports 2001 and 2002 PDD values calculated using summertime (June, July, August) temperatures, T, for all reanalysis data, as well as for the firn-core AWS. In order to remove bias in PDD values resulting from the higher-resolution sampling frequency, two values are presented for PDD calculations from the AWS site. The first value is calculated using 3 hourly averaged temperature data to have the same data resolution as the NARR eight-times-daily temperature data, while the bracketed values are calculated using 6 hourly averaged temperature data to have the same data resolution as the NCEP four-times-daily temperature data.

To find the most appropriate reanalysis dataset for the reconstruction of historical PDD values, we examine the correlation between summertime temperature records derived from the reanalysis datasets and the AWS temperature data for the same year. All of the reanalysis datasets

Table 2. Mean summertime (June–August) temperatures, T, and PDD values for the 2001 and 2002 firn-core AWS data, North American Regional reanalysis (NARR) data and US National Centers for Environmental Prediction (NCEP) reanalysis data. Correlation coefficients, R, between summertime temperatures from reanalysis data and firn-core AWS summertime temperatures for the same year are also shown. All of the reanalysis datasets correlate significantly with the firn-core AWS data at the 99% confidence level. The bias-corrected NCEP 850 mbar temperature (NCEP 850c T) data, shown in bold, were used to calculate historical PDD values

	T	R	PDD	
	°C		°C d	
2001				
Firn-core AWS	−4.1	1.00	24.3*	(23.3)[†]
NARR 2 m T	−4.7	0.76	10.0	
NCEP surface T	0.4	0.66	120.8	
NCEP 850 mbar T	−0.9	0.86	109.7	
NCEP 700 mbar T	−8.0	0.84	0.2	
NCEP 850c T[‡]	**−4.0**	**0.86**	**22.1**	
2002				
Firn-core AWS	−6.0	1.00	0.4*	(0.2)[†]
NARR 2 m T	−5.7	0.67	0.2	
NCEP surface T	0.3	0.58	92.4	
NCEP 850 mbar T	−3.0	0.78	30.0	
NCEP 700 mbar T	−10.3	0.73	0.0	
NCEP 850c T[‡]	**−6.1**	**0.78**	**1.0**	

*PDD values calculated using eight-times-daily AWS data.
[†]PDD values calculated using four-times-daily AWS data.
[‡]Bias-corrected temperature values. Calculated using the mean difference between mean AWS temperatures and mean NCEP pressure level temperature for both summers.

correlate significantly with the firn-core AWS data at the 99% confidence level. The NCEP 850 mbar T provides the highest correlation coefficient, R, with the firn-core AWS data for both years. However, as indicated by the mean temperature and PDD values, there is a systematic warm bias associated with this dataset. These data were bias-corrected using the mean difference in summertime temperatures for the two years and applying it uniformly across both datasets. These values are reported in Table 2 as NCEP 850c T (shown in bold). The NCEP 850c T was chosen for historical PDD reconstructions for the firn-core site because it provided the best correlation with the firn-core AWS, and, after bias correction, produced PDD values similar to those recorded at the firn-core AWS in both years.

Historic PDD values resulting from this analysis are used in the discussion below to link isotopic modification observed at the low-elevation snow-pit sites with the amount of isotopic modification expected to have occurred at the firn-core site in the past.

DISCUSSION

The processes that affect isotopic signals within a snowpack can be divided into open and closed systems. Open systems exchange mass with the surrounding environment, which can result in changes to the mean isotopic values. In the case of isotopic signals within the snowpack, these changes are most commonly due to the enrichment of the snowpack resulting from mass loss, where the light isotopes are preferentially removed from the snowpack via erosive
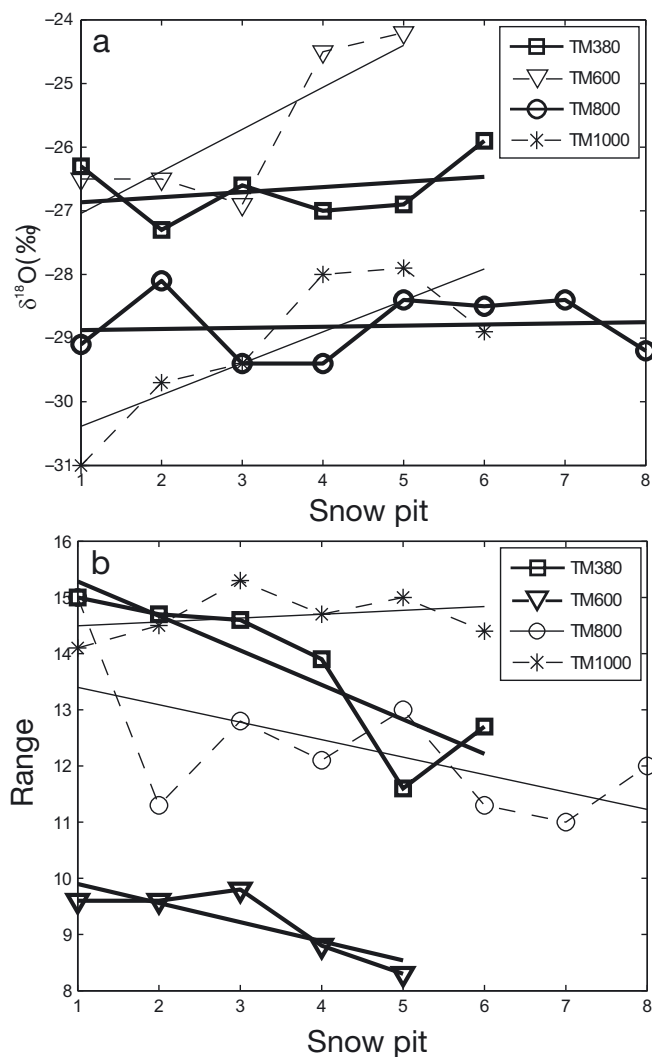
Fig. 8. Temporal changes in (a) mean $\delta^{18}O$ values and (b) $\delta^{18}O$ ranges (defined as the difference between the minimum and maximum $\delta^{18}O$ value within each snow pit) for all snow-pit sites.

sublimation (Stichler and others, 2001), evaporation (Moser and Stichler, 1975) or meltwater runoff (Árnason, 1969; Taylor and others, 2001). More enriched isotopic values can also be introduced into the snowpack in the form of springtime precipitation (Stichler and Schotterer, 2000).

Closed systems do not allow mass exchange with the surrounding environment, and thus average isotopic values are maintained while isotopic ranges (defined as the difference between the minimum and maximum $\delta^{18}O$ value within each snow pit) decrease. Homogenization of the snowpack and muting of the seasonal isotopic range can increase dating errors, particularly when chronologies rely on the layer counting of seasonal isotopic cycles (Koerner, 1997). Because closed-system processes do not alter average isotopic values, annual average temperature reconstructions are not affected. While purely closed systems are rare in natural environments, these conventions allow a convenient means to determine the dominant processes that modify isotopic ratios within snow pits, and consequently the degree of error associated with palaeotemperature reconstructions from sites experiencing isotopic modification.

Isotopic values

Linear-regression analysis is used to determine whether temporal changes in isotopic values are significant. All snow-pit sites experience an increase in average snowpack isotopic values over the course of the study (Figs 7 and 8a). We limit the influence of fresh snowfall over the course of our study by removing fresh snow samples from our analysis, but in some instances fresh snow may have melted into the underlying snowpack. This was most problematic at the TM600 and TM1000 snow-pit sites, where fresh snowfall had the largest percentage contributions, with up to 8% and 14%, respectively, of the total SWE at these sites coming from fresh snowfall. Fresh snow samples from these sites had average isotopic compositions of –22.4‰ and –21.1‰, respectively. We estimate the density of these samples as 200 kg m^{-3}, and calculate average isotopic enrichments of 0.3‰ and 1.1‰, respectively.

By contrast, fresh snow contributes 0.2% and 2% of the total SWE at TM380 and TM800, respectively. Fresh snow was not sampled at either of these sites, so average isotopic values from the TM600 and TM1000 fresh snow samples were used to estimate the average isotopic enrichments of <0.1‰ and 0.1‰ resulting from melting and percolation of fresh snow at TM380 and TM800. These effects are negligible at TM380 and TM800, but the increases in $\delta^{18}O$ values observed at TM600 and TM1000 may be heavily influenced by fresh snowfall inputs and are not included in the discussion.

Aeolian processes can also add snow to, or remove it from, snow-pit sampling sites. This potential source of error has been minimized by locating snow pits in close proximity to one another (i.e. by cutting snow-pit sampling walls back from one another). However, wind deposition was a concern at the TM600 sampling site where a hummocky glacial ice surface makes the region prone to both depositional and erosional processes within short distances of one another. This may explain the differences in stratigraphic profiles observed between the first two snow pits sampled at this site and the remaining pits (Fig. 7b), the lower than average isotopic ranges and the inconsistency in altitude effect observed at this site (Table 1). While wind redistribution is likely to have occurred at other snow-pit sites, the processes observed at these sites are believed to be more systematic.

The site that experienced the most melt, TM380, shows a significant decrease in isotopic range (Table 1; Fig. 8b), accompanied by an enrichment in $\delta^{18}O$ values. As can be seen from Figure 7a, minimum $\delta^{18}O$ values at TM380 do not experience a marked enrichment from the pre-melt snow-pit values until pit 5, between $h = 0.47$ and 0.62. Comparing this to the stratigraphy plots of Figure 4, pit 5, we see that meltwater percolated to a similar level ($h = 0.57$) in the snow-pit profile. TM800 shows similar results, where the depth of meltwater percolation corresponds to the changes in the isotopic profiles within the snowpack. Meltwater percolation is therefore considered the dominant process causing isotopic modification during the melt season.

Early in the melt season at TM380, reductions in isotopic range occur without a corresponding increase in mean $\delta^{18}O$ values, suggesting that closed-system processes dominate early-melt-season modification of isotopic stratigraphies. However, as the amount of meltwater in the system increases, open-system processes become increasingly important, as demonstrated by the enrichment of mean snow-pit $\delta^{18}O$ values during the latter part of the study period (Fig. 8a).

Because snow pits are an open system, there is potential for meltwater redistribution through both horizontal and vertical advection. Horizontal advection is assumed to have negligible effects on a snow pit's isotopic composition because water is able to migrate both into and out of the system. Ice-layer development was also finite and spatially limited over the course of the study, so we suspect that horizontal advection resulting from this process was minimal. However, in the ablation zone of glaciated systems vertical advection is assumed to be a net loss, as meltwater is lost to runoff, superimposed ice, evaporation or erosive sublimation. No meltwater or superimposed ice was observed at the base of any of the snow-pit sites, so evaporation and sublimation are thought to be the dominant processes influencing mass loss from these sites.

The role of ice layers in limiting mass exchange

Similar to the findings of Marsh and Woo (1984) and Conway and Benedict (1994), ice layers in our study formed at stratigraphic boundaries in the upper layers of the snowpack, with water spreading out laterally to form horizontal zones of saturation and ice layers. We did not sample these ice layers directly for density, but Marsh and Woo (1984) report densities ranging from 630 to 950 kg m^{-3}, with a mean value of 800 kg m^{-3} for ice layers formed in a Canadian Arctic snowpack.

These high-density, low-permeability layers near the surface of a snowpack are considered to be important in limiting the exchange of water vapour between the atmosphere and the snowpack (Zhou and others, 2008). As mentioned above, three out of the nine melt crusts observed in our snow-pit stratigraphies formed from the breakdown of ice layers during melt. While melt layers are denser than the surrounding snowpack, they represent a decrease in permeability from the antecedent ice layers. Thus the progression of the melt season and the consequent breakdown of impermeable ice layers into more permeable, loosely bonded melt crusts are thought to mark a significant transition in the factors controlling the modification of isotopic ratios within snowpacks, as these layers no longer limit exchange between the water vapour in the snowpack and the atmosphere. These findings are consistent with our results, where closed-system processes were found to dominate early in the melt season, with a transition to open-system processes as melt becomes more intense. While we did not directly measure vapour loss from the snowpack, the largest changes in mean $\delta^{18}O$ values occurred late in the study at TM380 (Fig. 8a). These changes are consistent with fractionation and loss of depleted vapour from the snowpack.

Isotopic modification

Two considerations are relevant to the degree of meltwater-induced isotopic modification experienced at a site: (1) the absolute amount of melt and (2) the per cent melt. In Arctic snowpacks that do not experience meltwater runoff, the dominant processes resulting in mass loss and isotopic modification are evaporation and sublimation (Stichler and others, 2001). Because these processes are largely restricted to the surface layers of a snowpack, the absolute melt may be the best predictor of isotopic modification because it is a measure of the amount of free water available for evaporation.

Alternatively, because annual temperature signals derived from ice cores are calculated from the entire year's

accumulation, it could be argued that the total melt is less important than the per cent melt. For example, high-melt years that also experience high annual accumulation may not experience a large degree of isotopic modification because a relatively small portion of the snowpack is affected by melt. In contrast, low-melt years that also experience low amounts of accumulation may experience relatively large amounts of isotopic modification as meltwater is able to penetrate through a significant portion of the snowpack.

Other factors likely to affect the degree of isotopic modification at a site include: (1) the timing, thickness and depth of ice-layer formation; (2) the timing, amount and phase of summertime precipitation; (3) the timing and intensity of summertime melt; (4) windiness; and (5) relative humidity. Further investigation of melt processes accounting for these factors is likely to increase our ability to quantify isotopic modification resulting from melt processes.

Linking melt amount and isotopic modification

PDD values and per cent melt amounts are used to link isotopic modification observed at the low-elevation snow-pit sites with isotopic changes at the firn-core site. The trends in $\delta^{18}O$ enrichment at TM380 and TM800 are not statistically significant; it is therefore recognized that these trends may prove to be negligible. However, these sites experienced a maximum PDD value of only 7.5°C d. Further study is therefore needed to determine whether this effect is real under higher-melt scenarios.

Degree-day factors (DDF, with units mm w.e. d^{-1} °C^{-1}) are used to relate PDD values to total melt. Arendt and Sharp (1999) calculated snow DDF at three different locations on John Evans Glacier, Ellesmere Island, with values ranging between 2.7 and 5.5 mm w.e. d^{-1} °C^{-1}. Because our study takes place at the beginning of the melt season when snow albedo is high, we use a relatively low DDF of 3.0 mm w.e. d^{-1} °C^{-1} to calculate the amount of ablation taking place at each snow-pit site over the duration of our study, as well as to estimate the amount of melt taking place at the firn-core site. These values are consistent with values for the Greenland ice sheet recommended by Braithwaite (1995).

Table 3 gives the SWE, PDD and absolute and per cent melt values calculated for each snow-pit sampling site as well as the historic values calculated for the firn-core site using NCEP 850c T data. Values presented for individual snow-pit sites were derived as follows: SWE was calculated directly from snow-pit depth and density measurements; PDD values were calculated from the temperature data collected at individual snow-pit sites over the course of the study; absolute melt amounts were calculated using PDD values from each snow-pit site and a DDF of 3.0 mm w.e. d^{-1} °C^{-1}; and per cent melt was derived using the methods of Fisher and Koerner (1994). Historical absolute and per cent melt values are derived from the NCEP 850c T dataset from 1967 to 2006 to span the time frame of the firn-core record and beyond. Accumulation values are measured from the firn-core stratigraphy, with the exception of 2000–01 and 2006 values, which come from snow-pit data. There are no accumulation data for 2003–05 at this site.

The historical melt record for the firn-core site (Fig. 9) indicates that 2001 was a high-melt year (66 mm w.e.), exceeded only by estimated melt values for 1998 (90 mm w.e.). Because of the lower accumulation observed in 2001, the per cent melt values for the two years are very similar, 33%

Table 3. Average historical SWE, PDD values, and total and per cent melt for the firn-core site. Absolute melt values for the firn-core site are derived from PDD values calculated using 1967–2006 NCEP 850c *T* data. Accumulation values are derived from the firn-core stratigraphy, except for values from 2000–01 and 2006, which came from snow-pit data. There are no accumulation data for 2003–05 for this site. SWE, PDD values, and absolute and per cent melt are shown for all snow-pit sampling sites

	SWE	PDD	Melt	Melt
	mm w.e	°C d	mm w.e	%
Firn core	295	10.0	29.9	10
TM380	125	7.5	22.5	18
TM600	118	5.5	16.5	14
TM800	126	3.7	11.1	9
TM1000	95	1.6	4.8	5

Fig. 10. Seasonal $\delta^{18}O$ signals at the firn-core drill site. These data indicate the persistence of seasonal $\delta^{18}O$ signals, even during years of intense melt, such as 2001.

and 36%, respectively. Compared with the historical per cent melt average of 10%, these two years have very high per cent melt values, >10% higher than the next highest melt year, 1999. Average summertime melt for the entire 40 year record is 30 mm w.e.

Figure 10 shows the isotopic signal from the top of the firn core, where it is clear that even during years of intense melt (e.g. 2001) the seasonal isotopic signals are preserved. Thus we are still able to identify and count annual layers. However, without calculations of melt, the likely enrichment of isotopic values observed in 2000–01 would be overlooked. Based on our snow-pit results, this would lead to an overestimation of annual temperatures derived for those years.

We assert that the preservation of annual isotopic signals is not an adequate indication of the preservation of isotopic values. This research indicates that isotopic signals subject to meltwater percolation experience, not only a reduction in seasonal isotopic range, but also an accompanying isotopic enrichment, most likely due to increased evaporation and sublimation. These changes result in overestimates in annual temperature records derived from sites that experience (even intermittent) intense melt events.
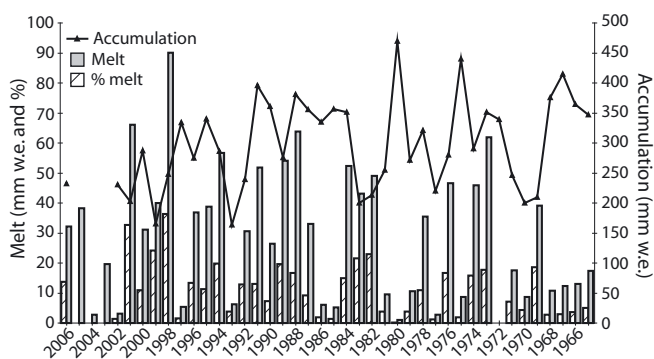
Table 3 indicates PDD values observed at individual snow-pit sites were not as high as those experienced at the firn-core drill site over the 40 year record. Linear relationships between PDD or per cent melt and isotopic modification are used to extrapolate between the amount of isotopic modification observed at the lower-elevation snow-pit sites and the firn-core site. These empirically derived linear relationships are based on the conservative estimates of isotopic enrichment observed at TM380, and are estimated to be $0.08‰(PDD)^{-1}$, with a PDD threshold of 2.5 days for the absolute melt scenario, and $0.03‰(\% \text{ melt})^{-1}$, with a threshold of 5% for per cent melt.

Linear extrapolation of these values is likely to underestimate temperature reconstruction errors, as there is thought to be a transition from closed- to open-system processes during the melt season which is more likely to result in an exponential relationship between melt amounts and isotopic modification, with an absolute threshold beyond which isotopic signals are lost. However, without the data to explore this assumption, we use the more conservative linear relationship between these variables.

In order to relate isotopic modification to temperature-error estimates, a $\delta^{18}O$–temperature relationship must be assumed. A broad range of $\delta^{18}O$–temperature relationships have been reported in the literature, with spatial slopes of $0.61‰(°C)^{-1}$ derived by Giovinetto and others (1997) for the eastern Canadian Arctic and $0.67‰(°C)^{-1}$ derived by Johnsen and others (1989) for West and South Greenland. However, because this study focuses on temperature reconstructions from a single site over time, a lower temporal slope is considered to be more appropriate. Temporal slopes reported by White and others (1997) for Greenland ice cores range between 0.16 and $0.54‰(°C)^{-1}$, with an average value of $0.31‰(°C)^{-1}$. Here we use a value of $0.54‰(°C)^{-1}$.

The isotopic modification factors presented above for absolute or per cent melt can be used to determine the average annual isotopic modification expected across the entire historical firn-core record or for individual years. The firn-core site has an average historical PDD value of 10.0°C d from 1967 to 2006, which translates into average annual isotopic modifications of 0.6‰. Using the temporal $\delta^{18}O$–

Fig. 9. Historical melt and per cent melt values for the firn-core site derived from PDD values calculated using 1967–2006 bias-corrected NCEP 850 mb *T* data. Accumulation values are derived from the firn-core stratigraphy, except for values from 2000–01 and 2006, which came from snow-pit data. There are no accumulation data for 2003–05 for this site. Average melt for the record is 30 mm w.e., mean per cent melt is 10% and average annual accumulation is 295 mm w.e.
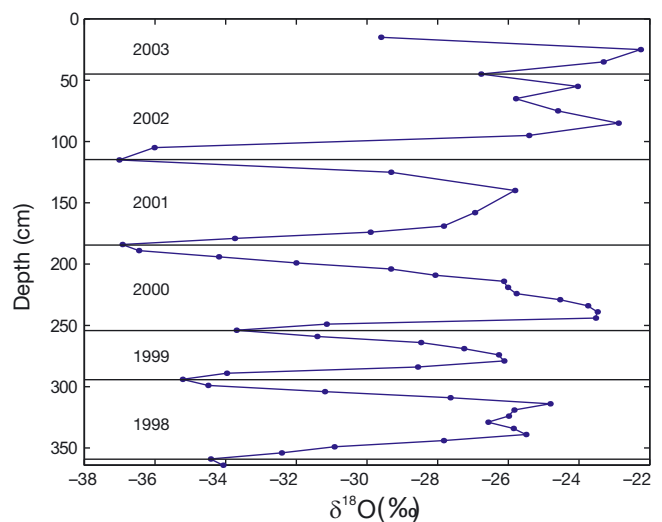
temperature relationship of $0.54‰(°C)^{-1}$ presented above, we estimate average annual temperature overestimations of $1.1°C$ for the firn-core site. If this relationship is extended to our highest-melt summers, 2001 and 1998, with PDD values of 22.0 and $30.0°C\,d$, respectively, isotopic enrichments of $1.5–2.2‰$ could be expected, introducing annual average temperature errors of $+2.7$ and $4.1°C$.

More conservative temperature-error estimates result if per cent melt values are used. These values result in an isotopic modification of $0.03‰(\%\,melt)^{-1}$, with a threshold of 5%. The 5% melt threshold is consistent with results presented by Koerner and others (1999), where chemical signals were well preserved in an ice core drilled in Agassiz Ice Cap, Ellesmere Island, with a melt index of $<5\%$. The average per cent melt value from 1967 to 2006 for the firn-core site is 10%. This translates into average annual isotopic modification of $+0.2‰$, resulting in an average annual temperature overestimation of $0.3°C$ for the firn-core site from 1967 to 2006. Isotopic enrichments of $+0.8–0.9‰$ would be expected if this relationship is extended to our high-melt years, 2001 and 1998, corresponding to average annual temperature overestimates of $+1.5$ and $1.7°C$, respectively.

Annual accumulation at the firn-core site decreases over the 40 year record from 1967 to 2006 (Fig. 9). These decreases are accompanied by increases in absolute and per cent melt amounts at the site. As a result of these trends, the amount of isotopic modification observed at the firn-core site is expected to also be increasing.

CONCLUSION

Increasing snow-pit temperatures at all four sampling sites are accompanied by increases in snow-pit density, grain size, water content and mean $\delta^{18}O$ values. The enrichment of $\delta^{18}O$ values is observed to coincide with the percolation of more enriched meltwater into the snowpack, an indication that, after fresh snowfall inputs have been accounted for, meltwater processes dominate isotopic modification during the early melt season.

Two snow pits were eliminated from our final analysis because we suspect that isotopic enrichments at these sites were significantly influenced by fresh snowfall inputs during the course of our study. Even with PDD values of $\leq 7.5°C\,d$ (Table 1), increases in isotopic values were observed at the remaining two snow-pit sites. As these trends were not statistically significant, it is acknowledged that the trend in $\delta^{18}O$ enrichment may prove to be negligible. However, further study is needed to determine whether this effect is real under higher-melt scenarios. If the effect is real then the amount of isotopic modification observed at the snow-pit sampling sites can be extended to a higher-elevation firn-core site on the same icefield using PDD or per cent melt values.

For the absolute melt scenario, we derive an isotopic modification factor of $0.08‰(PDD)^{-1}$, with a 2.5 PDD threshold. This results in average annual isotopic enrichments of $0.6‰$, or average annual temperature overestimates of $1.1°C$, for the firn-core site from 1967 to 2006. In the warmest years, 2001 and 1998, isotopic enrichments of $1.5–2.2‰$ could be expected, introducing temperature errors as high as $+4°C$.

An isotopic modification of $0.03‰(\%\,melt)^{-1}$, with a threshold of 5%, is derived for the per cent melt scenario, resulting in more conservative estimates of annual average temperature errors. This translates into an average annual isotopic modification of $0.2‰$, resulting in average annual temperature overestimations of $0.3°C$ for the firn-core site from 1967 to 2006. Enrichments of $0.8‰$ and $0.9‰$ are expected in the extreme warm years, 2001 and 1998, corresponding to temperature errors of $+1.5$ and $1.7°C$.

We do not have confidence in our estimates of the temperature effects, as the isotope–temperature relationship is unknown at our field site. Assuming that this relationship is similar to that of Greenland, temperature offsets of a few degrees Celsius are possible in warm years. The large interannual variability in melt extent (hence temperature offset) also complicates temperature reconstructions. Meltwater effects need to be further examined and quantified to better assess this potentially large impact on isotope thermometry. The predicted degree of isotopic enrichment should be readily measurable under high-melt scenarios.

REFERENCES

Arendt, A. and M. Sharp. 1999. Energy balance measurements on a Canadian high Arctic glacier and their implications for mass balance modelling. *IAHS Publ.* 256 (Symposium at Birmingham 1999 – *Interactions between the Cryosphere, Climate and Greenhouse Gases*), 165–172.

Árnason, B. 1969. The exchange of hydrogen isotopes between ice and water in temperate glaciers. *Earth Planet. Sci. Lett.*, **6**(6), 423–430.

Braithwaite, R.J. 1995. Positive degree-day factors for ablation on the Greenland ice sheet studied by energy-balance modelling. *J. Glaciol.*, **41**(137), 153–160.

Conway, H. and R. Benedict. 1994. Infiltration of water into snow. *Water Resour. Res.*, **30**(3), 641–649.

Dansgaard, W. *and 10 others*. 1993. Evidence for general instability of past climate from a 250-kyr ice-core record. *Nature*, **364**(6434), 218–220.

Denoth, A. 1994. An electronic device for long-term snow wetness recording. *Ann. Glaciol.*, **19**, 104–106.

Eller, H. and A. Denoth. 1996. A capacitive soil moisture sensor. *J. Hydrol.*, **185**(1–4), 137–146.

Fisher, D.A. and R.M. Koerner. 1994. Signal and noise in four ice-core records from the Agassiz Ice Cap, Ellesmere Island, Canada: details of the last millennium for stable isotopes, melt and solid conductivity. *Holocene*, **4**(2), 113–120.

Friedman, I., C. Benson and J. Gleason. 1991. Isotopic changes during snow metamorphism. *In* Taylor, H.P., Jr, J.R. O'Neill and I.R. Kaplan, *eds. Stable isotope geochemistry: a tribute to Samuel Epstein*. Washington, DC, Geochemical Society, 211–221. (Special Publication 3.)

Giovinetto, M.B., G. Holdsworth, D.A. Fisher, N.M. Waters and H.J. Zwally. 1997. An assessment of the regional distribution of the oxygen-isotope ratio in northeastern Canada. *Ann. Glaciol.*, **25**, 214–219.

Goto-Azuma, K., R.M. Koerner and D.A. Fisher. 2002. An ice-core record over the last two centuries from Penny Ice Cap, Baffin Island, Canada. *Ann. Glaciol.*, **35**, 29–35.

Grumet, N.S. *and 7 others*. 2001. Variability of sea-ice in Baffin Bay over the last millennium. *Climatic Change*, **49**(1–2), 129–145.

Johnsen, S.J., W. Dansgaard and J.W.C. White. 1989. The origin of Arctic precipitation under present and glacial conditions. *Tellus B*, **41**(4), 452–468.

Johnsen, S.J., H.B. Clausen, K.M. Cuffey, G. Hoffmann, J. Schwander and T. Creyts. 2000. Diffusion of stable isotopes in polar firn and ice: the isotope effect in firn diffusion. *In* Hondoh, T., *ed. Physics of ice core records*. Sapporo, Hokkaido University Press, 121–140.

Jouzel, J. *and 12 others*. 1997. Validity of the temperature reconstruction from water isotopes in ice cores. *J. Geophys. Res.*, **102**(C12), 26,471–26,487.

Koerner, R.M. 1997. Some comments on climatic reconstructions from ice cores drilled in areas of high melt. *J. Glaciol.*, **43**(143), 90–97.

Koerner, R.M., D.A. Fisher and K. Goto-Azuma. 1999. A 100 year record of ion chemistry from Agassiz Ice Cap, northern Ellesmere Island N.W.T., Canada. *Atmos. Environ.*, **33**(3), 347–357.

Marsh, P. and M.K. Woo. 1984. Wetting front advance and freezing of meltwater within a snow cover. 1. Observations in the Canadian Arctic. *Water Resour. Res.*, **20**(12), 1853–1864.

Marshall, S.J., M.J. Sharp, D.O. Burgess and F.S. Anslow. 2007. Near-surface-temperature lapse rates on the Prince of Wales Icefield, Ellesmere Island, Canada: implications for regional downscaling of temperature. *Int. J. Climatol.*, **27**(3), 385–398.

Moore, J.C., A. Grinsted, T. Kekonen and V. Pohjola. 2005. Separation of melting and environmental signals in an ice core with seasonal melt. *Geophys. Res. Lett.*, **32**(10), L10501. (10.1029/2005GL023039)

Moser, H. and W. Stichler. 1975. Deuterium and oxygen-18 contents as an index of the properties of snow covers. *IAHS Publ.* 114 (Symposium at Grindelwald 1974 – *Snow Mechanics*), 122–135.

Petit, J.R. *and 18 others*. 1999. Climate and atmospheric history of the past 420 000 years from the Vostok ice core, Antarctica. *Nature*, **399**(6735), 429–436.

Pfeffer, W.T. and N.F. Humphrey. 1996. Determination of timing and location of water movement and ice-layer formation by temperature measurements in sub-freezing snow. *J. Glaciol.*, **42**(141), 292–304.

Pohjola, V. *and 7 others*. 2002. Effect of periodic melting on geochemical and isotopic signals in an ice core on Lomonosovfonna, Svalbard. *J. Geophys. Res.*, **107**(D4), 4036. (10.1029/2000JD000149)

Schneebeli, M., C. Coléou, F. Touvier and B. Lesaffre. 1998. Measurement of density and wetness in snow using time-domain reflectometry. *Ann. Glaciol.*, **26**, 69–72.

Schotterer, U., W. Stichler and P. Ginot. 2004. The influence of post-depositional effects on ice core studies: examples from the Alps, Andes, and Altai. *In* Cecil, L.D., J.R. Green and L.G. Thompson, *eds. Earth paleoenvironments: records preserved in mid- and low-latitude glaciers*. Dordrecht, etc., Kluwer Academic, 39–60.

Solomon, S. *and 7 others, eds.* 2007. *Climate change 2007: the physical science basis. Contribution of Working Group I to the Fourth Assessment Report of the Intergovernmental Panel on Climate Change*. Cambridge, etc., Cambridge University Press.

Stichler, W. and U. Schotterer. 2000. From accumulation to discharge: modification of stable isotopes during glacial and post-glacial processes. *Hydrol. Process.*, **14**(8), 1423–1438.

Stichler, W., U. Schotterer, K. Fröhlich, P. Ginot, C. Kull and H.W. Gäggeler. 2001. The influence of sublimation on stable isotope records recovered from high altitude glaciers in the tropical Andes. *J. Geophys. Res.*, **106**(D19), 22,613–22,620.

Taylor, S., X. Feng, J.W. Kirchner, R. Osterhuber, B. Klaue and C.C. Renshaw. 2001. Isotopic evolution of a seasonal snowpack and its melt. *Water Resour. Res.*, **37**(3), 759–769.

Unnikrishna, P.V., J.J. McDonnell and C.C. Kendall. 2002. Isotope variations in a Sierra Nevada snowpack and their relation to meltwater. *J. Hydrol.*, **260**(1), 38–57.

Waldner, P., M. Schneebeli, U. Schultze-Zimmermann and H. Flühler. 2004. Effect of snow structure on water flow and solute transport. *Hydrol. Process.*, **18**(7), 1271–1290.

White, J.W.C. *and 7 others*. 1997. The climate signal in the stable isotopes of snow from Summit, Greenland: results of comparisons with modern climate observations. *J. Geophys. Res.*, **102**(C12), 26,425–26,439.

Zhou, S., M. Nakawo, S. Hashimoto and A. Sakai. 2008. The effect of refreezing on the isotopic composition of melting snowpack. *Hydrol. Process.*, **22**(6), 873–882.